# INFLUENCE OF INITIAL HOLE PREPARATION ON PROPERTIES AND LIMITS IN HOLE FLANGING

**JAN RIHACEK, VACLAV ZEJDA, EVA PETERKOVA, MICHELA CISAROVA**

Brno University of Technology, Faculty of Mechanical Engineering, Institute of Manufacturing Technology, Brno, Czech Republic

**DOI : 10.17973/MMSJ.2020_12_2020065**

**rihacek.j@fme.vutbr.cz**

The paper deals with an analysis of a hole flanging technology, especially with the influence of an initial hole production process on an ability of material to achieve the required expansion in the application for automotive industry, i.e.radius rod production. S420MC steel sheet with a thickness of 4 mm is used as a material for the production of flanged parts. In this case, the possibility of improving limits in hole flanging by shaving technology is investigated. Therefore, holes made by conventional punching, shaving and laser cutting are investigated, for further comparison, using so-called hole expanding test. Subsequently, test results are compared with the prediction based on numerical simulation model in PAM-Stamp software.

**KEYWORDS**

forming, flanging, numerical simulation, PAM-Stamp, hole expanding test, S420MC steel

## 1 INTRODUCTION

In today's trend of reducing weight, saving the amount of consumed material and reducing the cost of production, the flanging is a very progressive technology of sheet metal forming. It can be highly productive when using suitable tools and, due to useful properties of manufactured parts, also extremely effective. Thanks to the flanging technology, it is possible to achieve a significant increase in the stiffness and buckling stability of the part by increasing the quadratic moment of its cross-section. The use of the flanging also results in a significant reduction in weight while maintaining rigidity. The hems can be of various shapes and uses. Currently, major applications are mainly in the aerospace and automotive industries. [Forejt 2004], [Zejda 2020]

This is also the case with the application of flanging technology to the innovative production of the radius rod, which is part of the truck chassis. The solved design of the production technology is realized in cooperation with THK Rythm Automotive Czech, which is currently engaged in the production of radius rods in several variants of types and sizes. In principle, these are pressed silent blocks in machined forged or cast heads, which are connected by a thick-walled tube. Mentioned design is very robust and it has considerable weight too. Therefore, a new design was created, using two symmetrical cold-formed sheet metal parts. It is assumed that the stamped parts will be joined in three places. For the first connection, located in the middle part of the rod, the clinching technology will be used. The other two connections will be realized thanks to the shape adapted steel housings of the rubber silentblocks, which are pressed into the flanged holes of the stamped parts, see Fig. 1. [Sigmund 2019], [Zejda 2020]

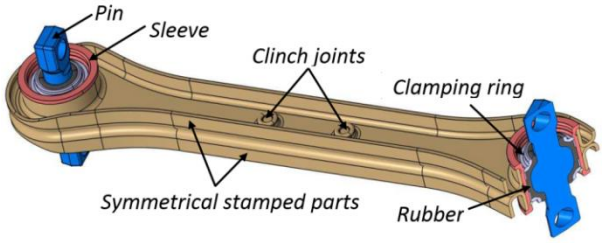


**Figure 1.** Concept of new radius rod design [Zejda 2020]

Since the radius rod is relatively highly dynamically stressed, it was necessary to choose an adequate material with good strength in terms of use, but also good formability in terms of production. Mentioned requirements for the blank material are met by hot-rolled steel sheet with a thickness of 4 mm, which is made of S420MC steel. Its chemical composition is shown in Tab. 1. [Zejda 2020]

| %C | %Mn | %Si | %P |
|---|---|---|---|
| max. 0.12 | max. 1.60 | max. 0.50 | max. 0.0025 |

| %S | %Al | %Nb | %V | %Ti |
|---|---|---|---|---|
| max. 0.015 | min. 0.015 | max. 0.09 | max. 0.20 | max. 0.15 |

**Table 1.** Chemical composition of S420MC steel [Zejda 2020]

For description of basic mechanical properties standard tensile tests were also performed for the material in the rolling direction at room temperature under a constant strain rate of $5 \cdot 10^{-3}$ $s^{-1}$ using a ZD 40 testing machine. A primary evaluation of recorded values was performed in M-TEST software. The resultant engineering stress – strain curve is shown in Fig. 2.

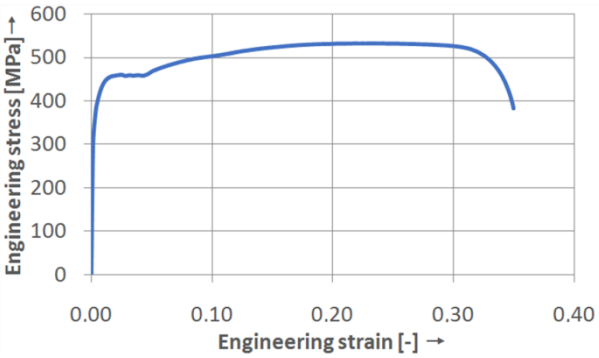


**Figure 2.** Engineering stress – strain curve of S420MC steel

Furthermore, an anisotropic effect of the S420MC steel was evaluated for different directions relative to the rolling direction (0°, 45° and 90°) for 20 % of the plastic strain. Coefficients of plastic anisotropy are tabulated in Tab. 2.

| | | | |
|---|---|---|---|
| Coefficient of plastic anisotropyfor 0° | $r_0$ | [-] | 0.741 |
| Coefficient of plastic anisotropy for 45° | $r_{45}$ | [-] | 1.011 |
| Coefficient of plastic anisotropy for 90° | $r_{90}$ | [-] | 0.659 |
| Mean coefficient of plastic anisotropy | $r_s$ | [-] | 0.856 |
| Yield stress ratio for for 0° | $\sigma_0$ | [-] | 1.000 |
| Yield stress ratio for for 45° | $\sigma_{45}$ | [-] | 1.007 |
| Yield stress ratio for for 90° | $\sigma_{90}$ | [-] | 1.071 |

**Table 2.** Mechanical properties of S420MC steel

The new design is conditioned by the production of flanges with diameter of 70 mm on both stamped parts. For this reason, it is necessary to determine the production limits, pecially the achievable flange height. Surely, numerical simulations can be used for this purpose. If the flanging options would not be suitable, other production technologies would have to be chosen, such as progressive drawing with punching or even 3D wire metal printing. [Sigmund 2019], [Zejda 2020]

The final value of the flange size is influenced by several factors. The quality of the initial hole surface has a dominant effect. It is also important what technology is used for production. Other factors influencing the flanging are mainly the mechanical properties of the material and then the geometry of the flange itself, contact friction, the stress state or factors associated with the thickness of the sheet, the shape of the punch, etc. Due to the number of factors that affect quality and manufacturability, an experimental evaluation was firstly performed, which can then be used for verification of the numerical simulation model.

## 2 THE HOLE FLANGING PROCESS

Conventional fixed tools are most often used for hole flanging. It is usually a combination of punch-die-blank holder, as it is shown in Fig. 3. In this case, the size of the gap 'z' between the punch and the die has a major effect on the shape of the resulting flange.

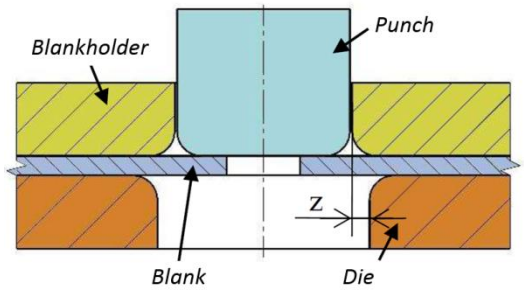


**Figure 3.** Arrangement of tools for circular hole flanging [Zejda 2020]

Examples of hole flanges are shown in Fig. 4. The shape according to Fig. 4a is formed in the case of the same gap size as the sheet thickness, Fig. 4b is formed with a gap greater than the sheet thickness and Fig. 4c shows the so-called bowl flange. [Zejda 2020]

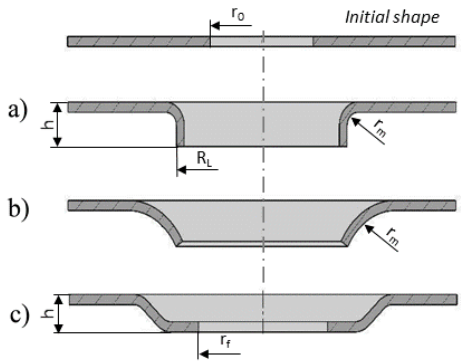


**Figure 4.** Examples of flange shapes [Zejda 2020]

Punches can have different end faces. The most common is a straight face with a rounded edge, but conical punches or punches with a spherical or traktrix end are also used.

In the intermediate phase of the flanging, the cylindrical flange is identical in shape to the bowl flange and its stress and deformation state is shown in Fig. 5. A biaxial stress state occurs in the area below the punch face, i.e. both stress components $\sigma_r$ and $\sigma_\theta$ are positive. In contrast, the deformation state is triaxial. The circumferential strain $\varepsilon_\theta$ is positive and of all strains it takes the highest values. In the radial direction, the material fibres are shortened and the strain $\varepsilon_r$ is therefore negative. In the sheet thickness direction, the strain $\varepsilon_t$ is also negative and thus thinning occurs. The greatest thinning occurs at the edge of the hole, where uniaxial stress state prevails.

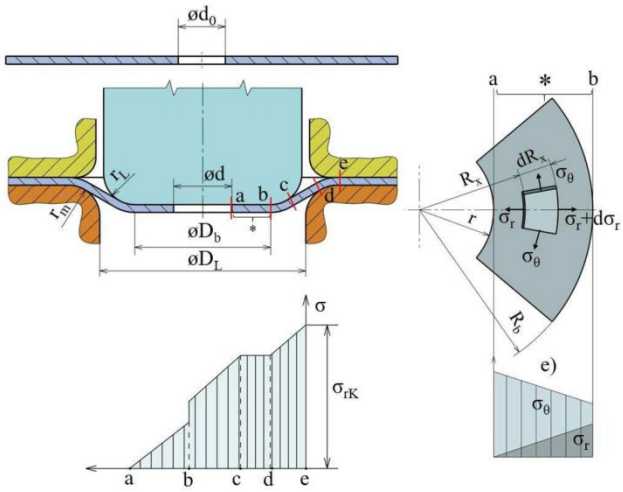


**Figure 5.** Stress state in flanging process [Zejda 2020]

Of course, the diameter of the hole cannot be determined simply by expanding the resulting shape of the flange. The law of volume conservation could be used, but for that we would need to know the function with which the thickness of the sheet changes depending on the movement of the punch. Due to the radial strain and action of other factors affecting the final height, such as the gap between the punch and the die, the shape of the punch, the material, etc., it is necessary to use empirical formulas. Literature [Gorbunov 1981], for example, states the following relationship:

$$D_0 = (D_L - t_0) + 0.86 \cdot r_m + 1.43 \cdot t_0 - 2 \cdot h \qquad (10)$$

where $D_L$ is the required inner flange diameter [mm] and h is the hem height [mm].

The application field of mentioned equation is limited by the range of $k_L$ and the large radii of the die edge $r_m$. A simplified relation can be used for very sharp radii and a tight gap, specifically:

$$D_0 = D_L - 2 \cdot h \qquad (11)$$

### 2.1 Hole expanding test

As it is already mentioned above, during expanding (flanging) of the hole, a uniaxial stress state, as in the tensile test, occurs near the free edge. The material is stressed near the hole only by the circumferential stress $\sigma_\theta$ and the radial stress $\sigma_r$ remains zero. The idea of comparing two stress states in terms of strain states is then obvious. Although it might seem that the results of the tensile test can be easily applied to the achievable strain values during the hole flanging, the opposite is true. It is also evident that the values of strains cannot be evaluated, for example, against the classical forming limit curve (FLC), which describes the material necking behavior. Currently, the hole expansion ratio (HER), defined by the hole expansion test (HET), is the most commonly used to evaluate the manufacturability of flanges:

$$HER = \frac{d_h - d_0}{d_0} \cdot 100 \qquad (12)$$

where $d_h$ is the diameter of the hole after cracking [mm] and $d_0$ is the initial diameter of the hole [mm].

Basic principle of HET is shown in Fig. 6. A conical tool with an apex angle of 60° and a diameter of at least 50 mm is pressed into the hole of the clamped test specimen, which is thus expanded. The recommended inner diameter of the die is at least 40 mm, but may be larger considering the expected final flange diameter. A value of 5 mm is recommended for the radius of the die. The test is stopped and evaluated in the event of an initial crack on the edge of the specimen. [Gu 2018], [Paul 2020]

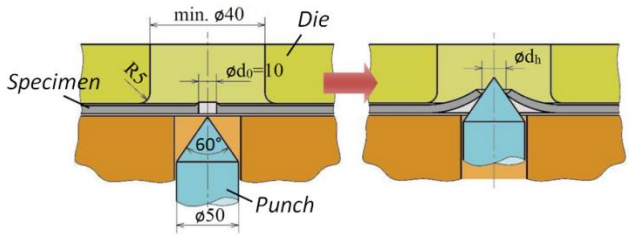


**Figure 6.** Basic principle of hole expanding test [Zejda 2020]

In [Gläsner 2016], for example, a modified method is described in which the HET and the so-called Kobe test (tensile test with punched circular hole) determine the maximum value of the principal strain, at which no cracks occur yet and the classical forming limit diagram (FLD) is extended by this value. In this case, acceptable strain values are not defined only by forming limit curve (FLC), but also by a horizontal line at the value of the maximum principal strain without cracking. This procedure is suitable for numerical simulations, but it is not practical for experimental analysis of defects on finished parts. It is applicable especially for linear strain paths in the area of tension-pressure. In order to be able to compare the achievable principal strains of different technologies, the same or as similar as possible state of the punched face of the expanded hole must be ensured. [Gläsner 2016]

Another way to use HET for hole edge failure prediction is to measure the thickness of the sheet near the crack, but far enough away that the measurement is not affected by the material necking. Measured thickness can be converted to relative thinning for determination of a safe value at which there is no risk of cracking. This procedure is applicable and easy assessable in numerical simulations, but especially useful in failure analyzes on real parts. The values of maximum thinning can also be achieved by recalculation directly from the measured HER values, assuming the volume conservation law and uniaxial stress state near the edge of the expanded hole according to the following relations [Hance 2013]:

$$r_s = \frac{\varphi_w}{\varphi_t} \approx \frac{\varphi_r}{\varphi_t} \tag{13}$$

where $r_s$ is themean coefficient of plastic anisotropy [-], $\varphi_w$ is the true strain in longitudinal direction of the specimen in tensile test [-], $\varphi_t$ is the true strain in the specimen thickness direction [-] and $\varphi_r$ is the true strain in the radial direction or minor true strain in the case of hole flanging [-].

$$\varphi_\theta = -\varphi_t \cdot (r_s + 1) \tag{14}$$

where $\varphi_\theta$ is the true circumferential strain or major true strain in the case of hole flanging [-].

$$\varphi_\theta = \ln\left(1 + \frac{HER}{100}\right) \tag{15}$$

$$\varphi_t = -\frac{\varphi_\theta}{r_s + 1} \tag{16}$$

It is now possible to define the engineering strain of the sheet thickness $\varepsilon_t$. As the sheet metal thins, the value is negative. By substituting the smallest measured value HER and R, it is possible to obtain the value of thinning, or ETL (edge thinning limit) [Hance 2013]:

$$-\varepsilon_t = ETL = 100 \cdot \left(1 - e^{\frac{\ln\left(1+\frac{HER_{min}}{100}\right)}{r_s+1}}\right) \tag{17}$$

## 3 EXPERIMENTAL DETERMINATION OF HER

ISO 16 630 standard defines a procedure for approaching the experimental determination of HER using hole expanding test. However, for example, the inner diameter and filleting radius of the die are not specified in the standard. Therefore, in many cases, the standardized method is adapted to conditions for the specific application. The size of the expanded hole was chosen to match the expected flange height in the case of solved production.

Considering achievable HER values, a series of 6 specimen types was designed. Each series contained specimens with holes made by laser cutting, single punching and double punching (shaving), due to anticipated production possibilities. The dimensions of the test specimen are shown in Fig. 7.

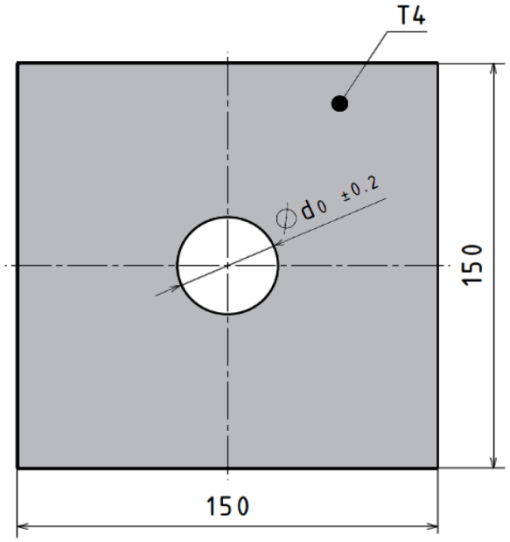


**Figure 7.** Specimen geometry

Because the final required flange diameter is larger than greater than the standardized tests given in the ISO standard, the test specimen also has larger dimensions. Namely, the hole diameters of 28, 32, 35, 40, 45 and 50 mm were used.

For experimental evaluation of HER, a test device was designed, which is shown in Figure 8. The device is adapted for UPM 600 tensile testing machine with hydraulic drive of the movable cross head. Testing machine dispose with maximum force of 600 kN. Loading speed was set to 10 mm · $min^{-1}$. The specimen is placed on the lower support plate. After applying the upper pressure plate, the specimen is centered against the draw edge using a centering ring and a conical punch with an apex angle of 60° and base diameter of 70 mm. Then, it is tightened with screws. The die insert diameter is 78 mm with edge rounding of 5 mm.

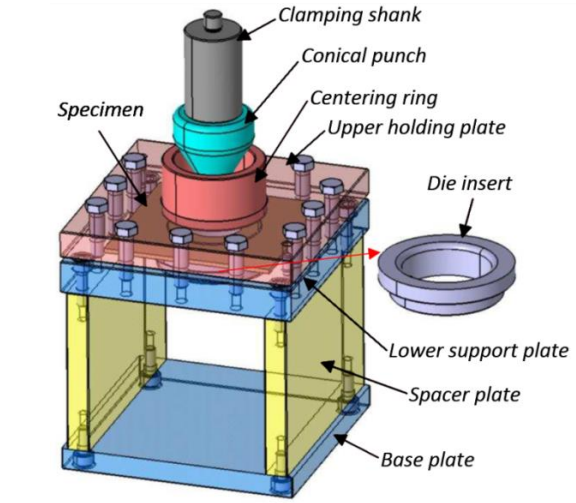


**Figure 8.** HER testing device [Zejda 2020]

The forming was captured through a mirror by a digital camera, which was connected to a laptop, so that the formation of the first crack passing through the entire thickness of the specimen could be observed, see Fig. 9.

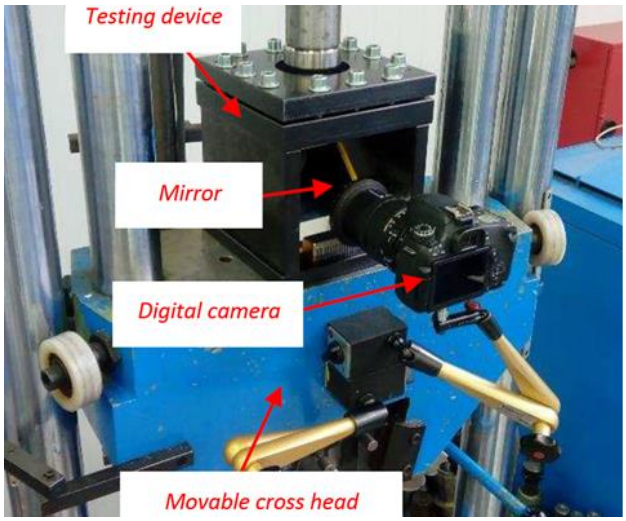


**Figure 9.**Testing device placed in the machine [Zejda 2020]

### 3.1 Specimens with Holes Made by Punching

In the first series of tests, specimens with holes prepared by punching were tested. Before each test, the hole diameter was measured in two directions perpendicular to each other. After the test, hole dimensions were measured in four directions, rotated by 45° relative to each other. In both cases, the measurement was performed with a digital caliper with a resolution of 0.01 mm. Since the emphasis was placed on the quality of the punched surface, at the expense of the shear force, less than the usual shear clearance was used during the hole punching process, i.e. 0.12 mm. A summary of results of punched specimens is given in Tab. 3. Each HER value was obtained by averaging of the results from three tested specimens.In addition to HER values, principal strains and edge thinning limit (ETL) values were also determined based on formulas (14) to (16).

| $\varnothing d_0$ | [mm] | 28.0 | 32.0 | 35.0 | 40.0 | 45.0 | 50.0 |
|---|---|---|---|---|---|---|---|
| HER | [%] | 23.2 | 22.1 | 21.5 | 22.2 | 22.5 | 23.5 |
| ETL | [%] | 13.4 | 13.0 | 12.4 | 12.8 | 13.0 | 13.6 |
| $\varphi_t$ | [-] | -0.112 | -0.108 | -0.105 | -0.108 | -0.109 | -0.114 |
| $\varphi_\Theta$ | [-] | 0.209 | 0.200 | 0.195 | 0.200 | 0.203 | 0.211 |
| $\varphi_r$ | [-] | -0.096 | -0.092 | -0.090 | -0.092 | -0.094 | -0.097 |

**Table 3.** Results of HET for holes made by punching

The hole expansion to the required dimension of 70 mm did not go without cracks in all cases. Furthermore, in the case of punched holes, cracks did not always occur in the same orientation with respect to the rolling direction. An example of through cracks in the specimen after the test is shown in Fig. 10.

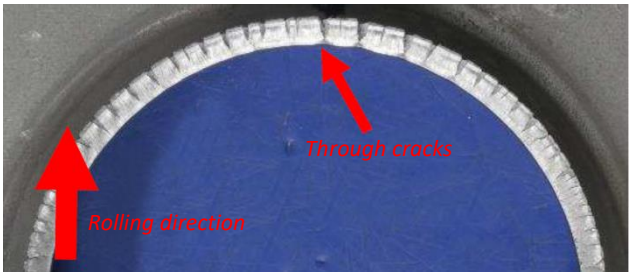


**Figure 10.** Punched surface after the test for initial diameter of 35 mm

### 3.2 Specimens with Holes Made by Shaving

In the next, specimens with holes prepared by shaving were tested.The specimens were prepared on the basis of pre-punched holes, from which the material, i.e. a ring with a wall thickness of approx. 0.5 mm, was punched in the second calibration step using the same clereance as in the prievous step. The aim was to make the same dimensions by the shaving as in the previous case. Before starting the test itself, a comparison of the punched surfaces was performed, see Fig. 11 and Fig. 12.

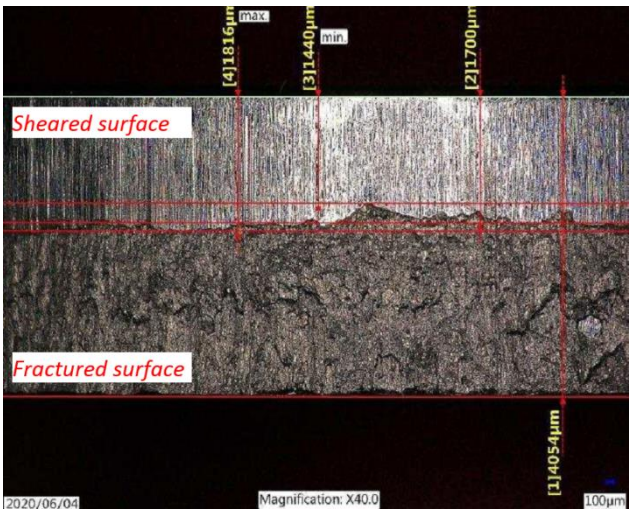


**Figure 11.** Example of punched surface after single punching process

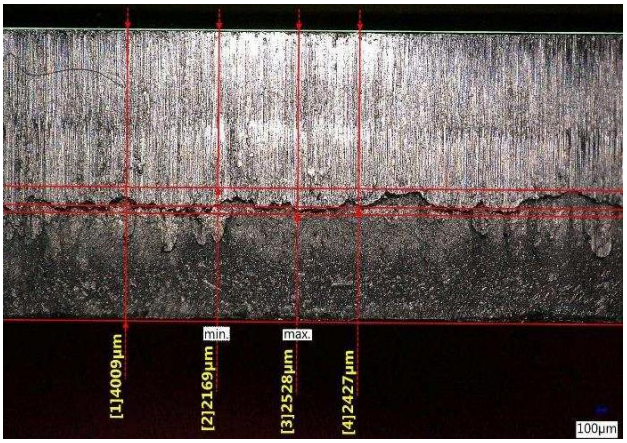


**Figure 12.** Example of punched surface after shaving process

As it is evident form the figures above, the fractured surface with worse quality was reduced by about 40 % thanks to shaving.

In addition, hardness measurements were also performed on a DuraScan hardness tester according to the Vickers method

with a load of 9.8 N. The measurement was performed in the direction from the punching edge to an unaffected base materialat a distance of 1.5 mm from the specimen surface. The results are shown in Fig. 13. It is important to note that the hardness values for once and twice punched specimen do not significantly differ.

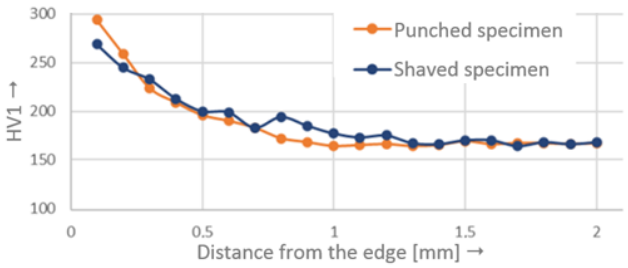


**Figure 13.** Hardness measurement results for punched and shaved specimen [Zejda 2020]

After performing HET, HER values and thus also ETL values are expected to increase. In the case of initial diameters of 45 and 50 mm, holes were expanded to the required diameter of 70 mm without cracking. A results summary of shaved specimens is shown in Tab. 4.

| ød$_0$ | [mm] | 28.0 | 32.0 | 35.0 | 40.0 | 45.0 | 50.0 |
|---|---|---|---|---|---|---|---|
| HER | [%] | 65.3 | 61.0 | 58.5 | 60.2 | 55.0 | 40.5 |
| ETL | [%] | 35.4 | 33.2 | 32.0 | 32.8 | 30.2 | 22.7 |
| $\varphi_t$ | [-] | -0.271 | -0.257 | -0.248 | -0.254 | -0.236 | -0.183 |
| $\varphi_\Theta$ | [-] | 0.503 | 0.476 | 0.461 | 0.471 | 0.438 | 0.340 |
| $\varphi_r$ | [-] | -0.232 | -0.220 | -0.212 | -0.217 | -0.202 | -0.157 |

**Table 4.** Results of HET for holes made by shaving

It should be noted that the values in tab. 4 are the averages again and the individual specimens showed each otherrelatively large variance. However, the beneficial effect of the shaving on the ability of the material to expand the hole is therefore undoubted. A comparison of two samples with the the initial hole diameter $d_0$ = 45 mm is shown in Fig. 14.

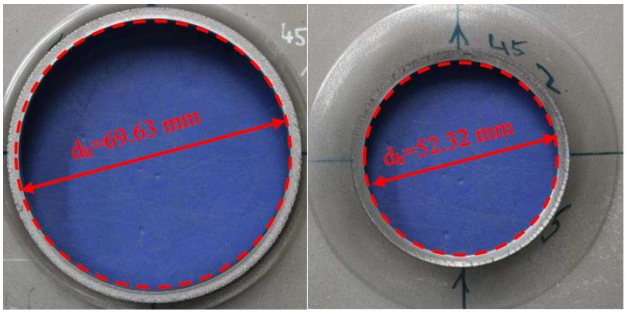


a) shaved hole b) punched hole

**Figure 14.** Comparison of achieved diameter of the expanded hole for shaving and simple punching

### 3.3 Specimens with Holes Made by Laser

Finaly, the last set for HET was consisted of specimens with holes prepared by laser cutting. A summary of the results of the laser cut specimens is given in Tab. 5

| ød$_0$ | [mm] | 28.0 | 32.0 | 35.0 | 40.0 | 45.0 | 50.0 |
|---|---|---|---|---|---|---|---|
| HER | [%] | 139.5 | 116.2 | 98.3 | 73.1 | 54.8 | 38.9 |
| ETL | [%] | 60.1 | 51.5 | 44.6 | 34.4 | 26.5 | 19.4 |
| $\varphi_t$ | [-] | -0.471 | -0.415 | -0.369 | -0.296 | -0.235 | -0.177 |
| $\varphi_\Theta$ | [-] | 0.873 | 0.771 | 0.685 | 0.549 | 0.437 | 0.329 |
| $\varphi_r$ | [-] | -0.403 | -0.356 | -0.316 | -0.253 | -0.202 | -0.152 |

**Table 5.** Results of HET for holes made by laser

The cracks occurred just before the hole extension to 70 mm for the size of the initial holes $d_0$ = 28 mm, which corresponds to the final average inner diameter of 67.3 mm and the flange height of 23.4 mm. Initial diameter of 32 mm can be considered as a limit value. Cracks did not occur until the end of the flanging, when the required diameter was reached. However, the other results are thus unimportant and rather informative. The specimen after the test is shown in Figure 15.

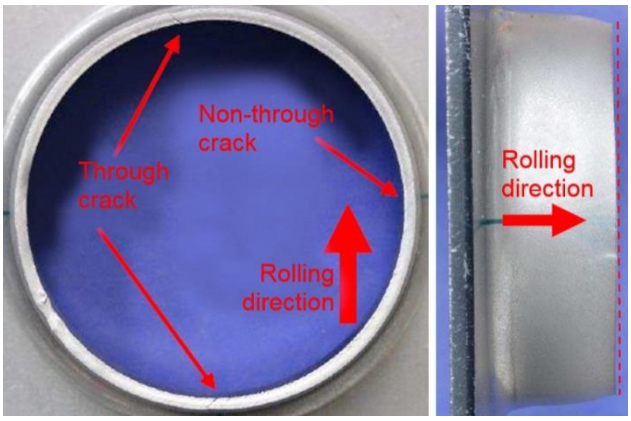


**Figure 15.** Final flange shape for initial diameter 28 mm

Compared to the previous hole making methodology, laser cutting shows incomparably better results in HER. The crack is located in line with the rolling direction. Fig. 16 shows a detail of one of the through cracks.

**Figure 16.** Detail of through crack for initial diameter 28 mm

## 4 NUMERICAL SIMULATION

The numerical simulation solution of the flanging process uses the finite element method. For this purpose, PAM-Stamp software was used. Firstly, a hardening curve of the formed material (see Fig. 2) was converted to the coordinates of true stress-true strain curve. Anisotropic propperties were described according to the Vegter lite model that uses Bezier interpolation function to describe the yield locus according to [Vegter 2011]. By measuring the reference points at different angle tothe rolling direction (0°, 45° and 90°), fully yield locus is determined using Vegter lite yield criterion, see Fig. 17.

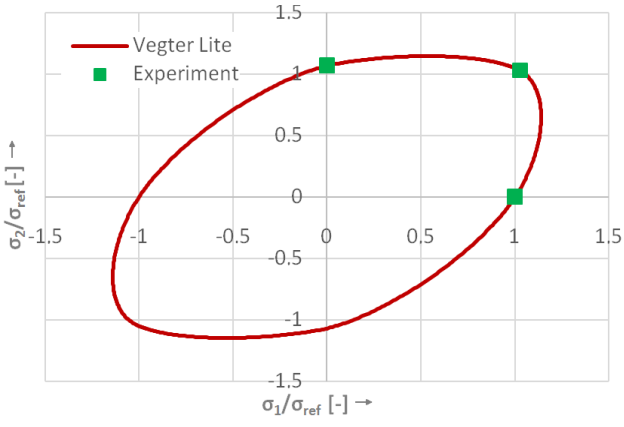


**Figure 17.**Vegter lite model for S420MC steel

The geometric model of the simulation corresponds to the testing device from Fig. 9. The tools were defined as ideally rigid, i.e. only contact elements are used. Solid mesh, resp. hexahedrons with an edge length of 1 mm, was used for specimen geometry description. If a shell mesh was used, the simulation would not give relevant results for this case.
It is clear that the numerical simulation does not exactely affect the influence of the material hardenning near the edge of the punched hole. For that reason, results of experiments that determine the deformation limit values for the numerical model are valuable. To compare the results, the diameter of the expandedd hole of 32 mm was chosen.

### 4.1 Specimens with Holes Made by Punching

Fig. 18. shows the distribution of the plastic equivalent strainalong the cross section of the test specimen when the inner flange diameter of 39.2 mm is reached, which corresponds to the experimentally determined maximum value.

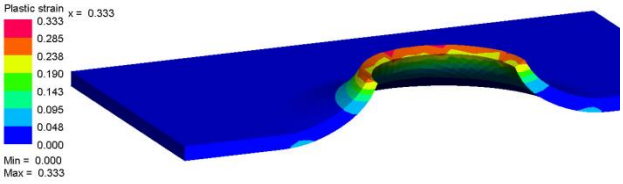


**Figure 18.** Distribution of the true plastic equivalent strain for expanded diameter of 39.2 mm

For a more accurate evaluation of the agreement between the simulation, the theory and the experiment, the variation of principal strains will be evaluated. Fig. 19, 20 and 21 show the variation of principal true strains as a function of the distance from the hole center of the specimen. These are mean values of cross sections in three main directions (0°, 45° and 90° toward the rolling direction). The results for the mentioned directions differ from each other by approximately 3 %, which is caused by anisotropic properties.

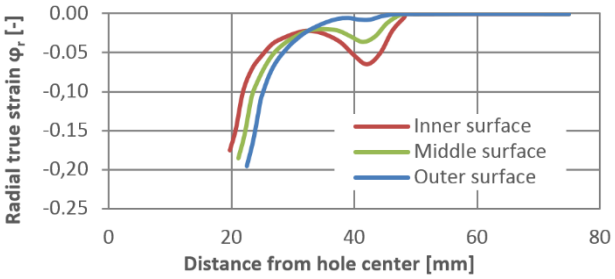


**Figure 19.** Variation of the radial true strain as a function of the distance from the specimen center for expanded diameter of 39.2 mm

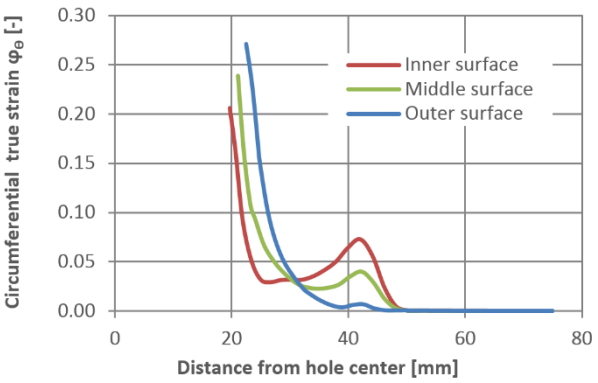


**Figure 20.** Variation of the circumferential true strain as a function of the distance from the specimen center for expanded diameter of 39.2 mm

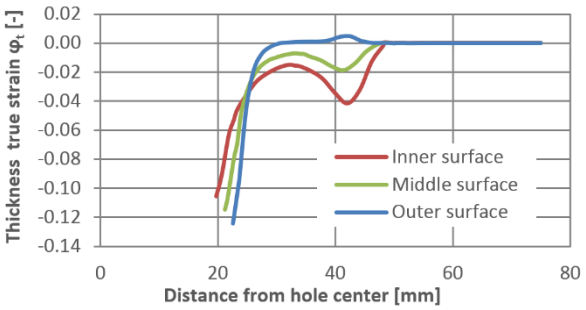


**Figure 21.** Variation of the thickness true strain as a function of the distance from the specimen center for expanded diameter of 39.2 mm

### 4.2 Specimens with Holes Made by Shaving

In the case of 32 mm diameter holes prepared by shaving, a maximum expansion value of 51.3 mm was found experimentally. For this state, the distribution of the plastic strain is also presented in Fig. 22.

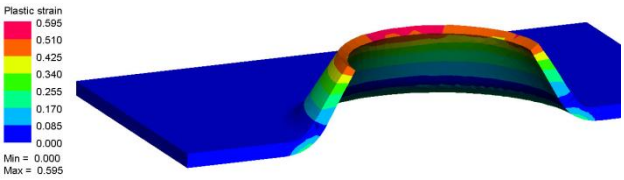


**Figure 22.** Distribution of the true plastic equivalent strain for expanded diameter of 51.3 mm

Even in this case, the curves of main strains were compared. Results for inner, middle and outer surface of the deformed specimen are shown in Fig. 23, 24 and 25.

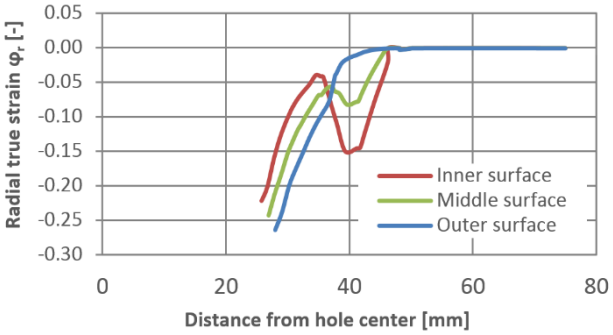


**Figure 23.** Variation of the radial true strain as a function of the distance from the specimen center for expanded diameter of 51.3 mm

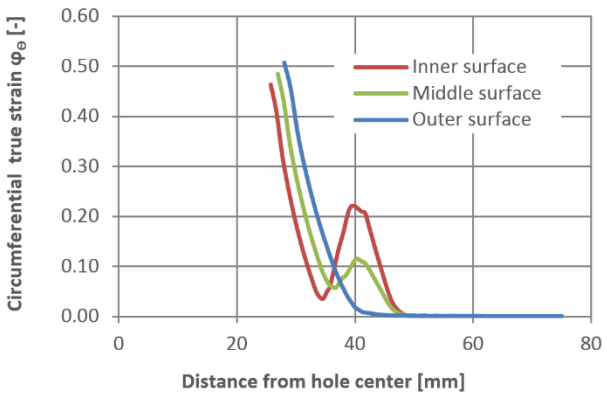


**Figure 24.** Variation of the circumferential true strain as a function of the distance from the specimen center for expanded diameter of 51.3 mm

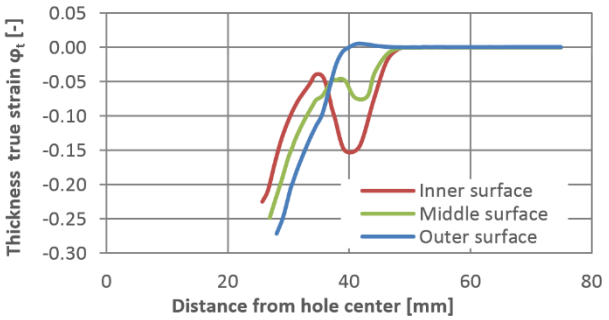


**Figure 25.** Variation of the thickness true strain as a function of the distance from the specimen center for expanded diameter of 51.3 mm

### 4.3 Specimens with Holes Made by Laser

For the initial hole diameter of 32 mm made by laser cutting, the experimantaly evaluated maximum value of expanded hole closely corresponds to the final diameter of the punch, i.e. 69.2 mm. Fig. 26 shows the simulation result with the distribution of the plastic strain.

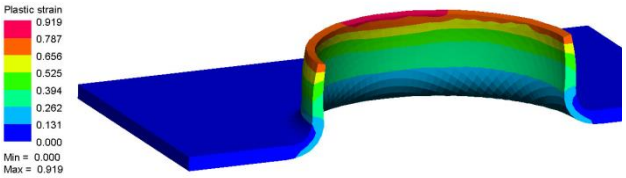


**Figure 26.** Distribution of the true plastic equivalent strain for expanded diameter of 69.2 mm

However, as in two previous cases, the distribution of principal strains along the cross section of the specimen was investigated, see Fig. 27, 28 and 29.

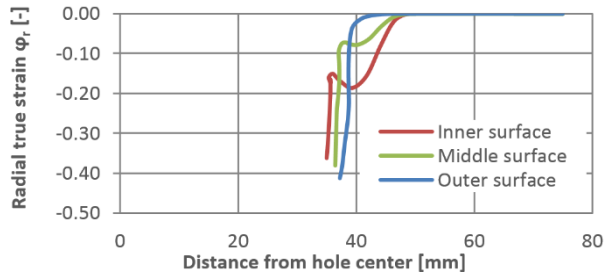


**Figure 27.** Variation of the radial true strain as a function of the distance from the specimen center for expanded diameter of 69.2 mm

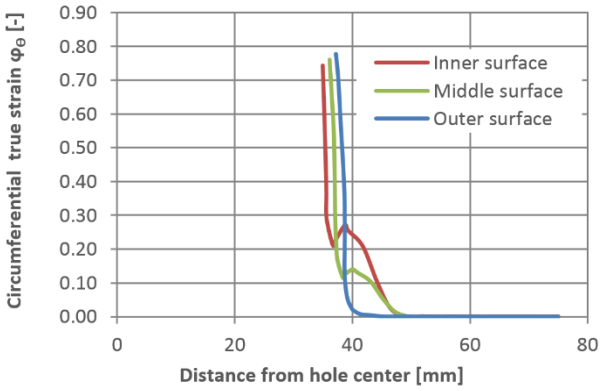


**Figure 28.** Variation of the circumferential true strain as a function of the distance from the specimen center for expanded diameter of 69.2 mm

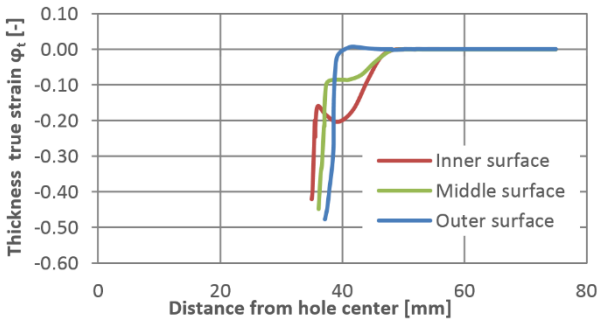


**Figure 29.** Variation of the thickness true strain as a function of the distance from the specimen center for expanded diameter of 69.2 mm

### 4.4 Results Comparison

After determination of the major and minor strain in chapter 3, it is possible to compare the determined limit values with the forming limit curve, which was experimentally found for the S420MC steel using the Nakajima test, see Fig. 30.

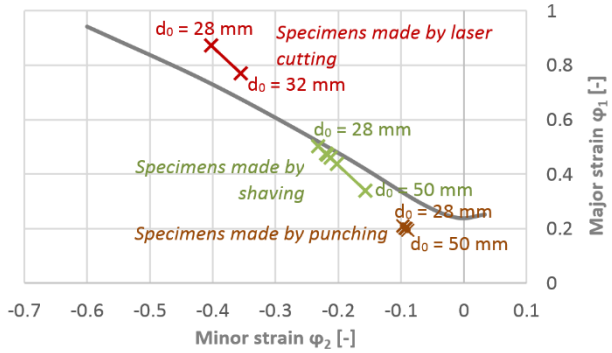


**Figure 30.** Comparison of experimentally determined principal true strains

It is clearly evident from the graph that detected limits do not correspond to the commonly used FLC. For the correct assessment of formability, it is therefore necessary to use the newly determined limit values. Further, it can be noted that the punched holes show the worst expending possibilities, according to the assumptions. If the shaving method is used in the production of the hole, the surface quality will increase and thus the limit strains will increase too, which is closer to the detected FLC. In the case of initial diameter of 28 mm, the strain limit state is increased by approx. 40 % if the shaving method is used. However, both methods lag behind laser cutting, which shows an even better limit state than predicted FLC.Furthermore, it can be stated that almost pure uniaxial tensile strain state ($\varphi_\Theta = -2 \cdot \varphi_r$) is occured at the hole edge during the hole expansion process for each variant. In addition, a comparison of the simulation results and experimentally determined and calculated values for the initial specimen hole diameter of 32 mm is shown in the graph in Fig. 31.

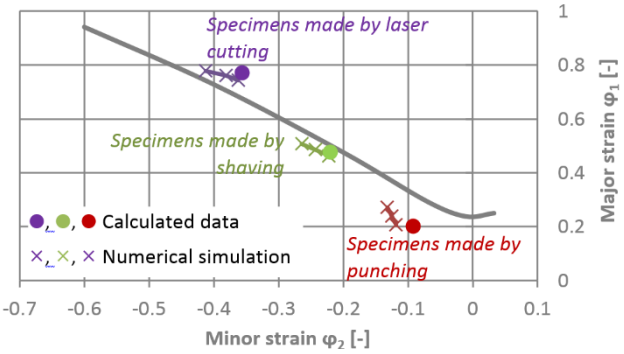


**Figure 31.** Comparison of experimentally determined and numerically predicted principal true strains for $d_0$ = 32 mm

In the graph, it is possible to observe a good degree of agreement between the simulation and the values obtained by the calculation based on experimental data. The greatest agreement is always reached for the values on the inner edge of the expanded hole, where the deviation between the numerical model and the calculated data is not higher than 3 %. In terms of material thinning comparison, three approaches were compared: numerical simulation results, values calculated according to equation (16) and experimental approach using measuring by micrometer. The determined values of maximum thinningare tabulated in Tab. 6 for the specimen with initial diameter of 32 mm.

| | Punched hole | Shaved hole | Laser cut hole |
|---|---|---|---|
| Numerical simulation | 21.5 % | 22.5 % | 35.8 % |
| Calculated values | 11.4 % | 29.3 % | 33.9 % |
| Experimental data | 15.7 % | 31.3 % | 42.3 % |

**Table 6.** Comparison of maximal percentagethinning values for initial diameter of 32 mm

The results show a very small agreement between experimentally measured and calculated data for specimen with laser cut hole, namely a difference of 8.4 % between the calculated and experimentally measured data, which is on the verge of technical acceptability. However, for smaller expansion ratios, the results show better agreement, namely maximal difference of 5.8 % in the case of punched hole (expanded hole diameter of 39.2 mm) and 6.8 % for the case of shaved hole (expanded hole diameter of 51.3 mm). Therefore, the model is applicable, especially for lower expansion ratios. For the case of the initial diameter of 32 mm, the forming force can be also compared, see Fig. 32.

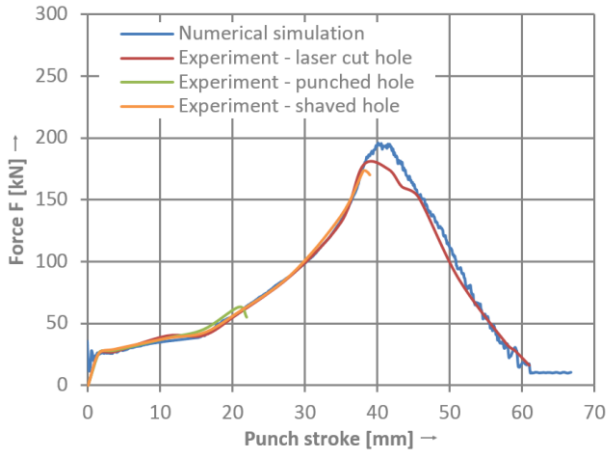


**Figure 32.** Comparison of experimentally determined and numerically predicted force – stroke diagrams for specimens with $d_0$ = 32 mm

There is no significant difference between the resulting force curves. The force at the beginning of the measurement firstly increases sharply. In this section, there is only edge contact between the material and the punch and a spatial bend of the formed material over the diecurvature. At the point where the force starts to grow steeper and the material abuts on the tool over a larger area, the hole expands faster and the material moves along the surface of the punch towards its cylindrical part. The force reaches its maximum even before the hole expands to the required dimension. During the whole time, measured data are in good agreement with the simulation, but there is a larger difference at the top of the curve, namely 8.8 %.

## 5 CONCLUSIONS

In this paper, the influence study of the initial hole production process on an ability of material to achieve the required expansion was performed. The analysis was based on the need to ensure the hole flanging and to determine the limits for S420MC steel with a thickness of 4 mm in the specific automotive application. Therefore, holes with various initial diameters 28 mm to 50 mm, which were made by conventional punching, shaving and laser cutting, are investigated, for further comparison, using so-called hole expanding test.

The HET results clearly showed an increase in the flange formability when using shaving technology instead of just punching, up to approximately 40 % of HER. However, both compared technologies do not reach the qualities of laser cutting, where only initial diameter of 28 mm has failed. On punched or shaved holes, cracks in all initial diameters were always appeared before the end of flanging process.

Subsequently, the critical values of the principal strain were determined by HER recalculation. The mentioned results were confronted with numerical simulation in the PAM-Stamp software. In the case of thinning, results were also compared with experimental evaluation. This also proved, among other things, the functionality of the numerical model and its acceptable accuracy.

It can be noted that on the basis of performed experiments and subsequent calculations, new forming limits applicable to each of three test cases were determined, which, in the case of the FLD use, do not match the predicted FLC. It is therefore necessary to consider the newly identified limits for the correct analysis of the flanging operations.


## ACKNOWLEDGMENTS

The paper was supported by project "Analysis of formability and weldability of materials produced by 3D wire metal printing" within the specific research of Faculty of Mechanical Engineering, Brno University of Technology relating to the grant no. FSI-S-20-6336 and with additional support of cooperation between Brno University of Technology, Faculty of Mechanical Engineering and THK Rythm Automotive Czech.


## REFERENCES


[Forejt 2004] Forejt, M. et al. Estabilishing the dynamic mechanical properties of materials by the hopkinson test method. Acta Mechanica Slovaca, 2004, Vol. 8, No. 2b,pp 93-98, ISSN: 1335-2393

[Glasner 2016] Glasner, T. et al. Considering the edge-crack sensitivity of a hot-rolled steel in forming simulation. In: Challenges in Forming High-Strength Sheets, Linz, 12–15 June, 2016, Bristol: IOP Publishing,pp 1-17, ISSN 0148-7191

[Gorbunov1981] Gorbunov, M. N. Sheet metal forming technology in the aerospace industry. Moscow: Machinery, 1981.(In Russian)

[Gu 2018] Gu, J. C. et al. A Practical Methodology to Evaluate and Predict Edge Cracking for Advanced High-Strength Steel. In: International Deep Drawing Research Group 37th Annual Conference, Waterloo, 3-7 June, 2018, IOP Conference Series: Materials Science and Engineering, 2011, Vol. 418, No. 1,pp 85-92, ISSN 1960-6206

[Hance 2013] Hance, B. et al. The Influence of Edge Preparation Method on the Hole Expansion Performance of Automotive Sheet Steels. SAE Technical Papers, April 2013, pp 1-12, ISSN 0148-7191

[Paul2020] Paul, S. K. A critical review on hole expansion ratio. Materialia, March 2020, Vol. 9, No. 1, pp 1-12, ISSN 2589-1529

[Sigmund 2019] Sigmund, M. Plasma overlay welding of cobalt alloy.MM Science Journal, October 2019, Vol. 2019, No. 3, pp 2982-2986. ISSN 1803-1269

[Vegter 2011] Vegter, H. et al. The Vegter Lite material model: simplifying advanced material modelling. International Journal of Material Forming, 2011,Bristol: IOP Publishing,pp 85-92, ISSN 1757-899X

[Zejda 2020] Zejda, V. Proposal of production technology of uni-axial rod. Brno: Brno University of Technology, 2020. (In Czech)

**CONTACTS:**
Ing. Jan Rihacek, Ph.D., Ing. Vaclav Zejda, Ing. Eva Peterkova, Ph.D., Ing. Michela Cisarova, Ph.D.
Brno University of Technology, Faculty of Mechanical Engineering, Institute of Manufacturing Technology, Department of Metal Forming
Technicka 2896/2, Brno, 616 69, Czech Republic
e-mail: rihacek.j@fme.vutbr.cz